Neurochemical Research (2019) 44:2156–2169
https://doi.org/10.1007/s11064-019-02855-9

ORIGINAL PAPER

Uptake of Intact Copper Oxide Nanoparticles Causes Acute Toxicity in Cultured Glial Cells

Arundhati Joshi[1,2] · Karsten Thiel[3] · Kshitija Jog[1] · Ralf Dringen[1,2]

Received: 12 June 2019 / Revised: 29 July 2019 / Accepted: 3 August 2019 / Published online: 14 August 2019

Abstract

Copper oxide nanoparticles (CuO-NPs) dispersions are known for their high cell toxic potential but contaminating copper ions in such dispersions are a major hurdle in the investigation of specific nanoparticle-mediated toxicity. In order to distinguish between the adverse effects exhibited by CuO-NPs and/or by contaminating ionic copper, the membrane-impermeable copper chelator bathocuproine disulfonate (BCS) was added in a low molar ratio (20% of the total copper applied) in order to chelate the copper ions that had been released extracellularly from the CuO-NPs before or during the incubation. Physicochemical characterization of synthesized CuO-NPs revealed that the presence of this low concentration of BCS did not alter the size or zeta potential of the CuO-NPs. Application of CuO-NPs to C6 glioma cells and primary astrocytes induced a concentration- and temperature-dependent copper accumulation which was accompanied by a severe loss in cell viability. The adverse consequences of the CuO-NP application were not affected by the presence of 20% BCS, while the copper accumulation and cell toxicity observed after application of ionic copper were significantly lowered in the presence of BCS. These results demonstrate that for the experimental conditions applied the adverse consequences of an exposure of cultured glial cells to dispersions of CuO-NPs are mediated by accumulated NPs and not caused by the uptake of contaminating copper ions.

Keywords Astrocytes · Copper · Glia · Nanoparticles · Toxicity

Introduction

Copper-containing nanoparticles (NPs) have gained substantial interest due to their unique properties which make them interesting materials for technical, pharmaceutical and biomedical applications, including processes such as organic waste treatment and antibacterial protection [1–3]. However, in vitro studies on a number of different cell types [4–6], including some types of glial cells [7, 8], have clearly demonstrated the toxic potential of copper-containing NPs. This has in fact stimulated studies regarding the potential use of copper-containing NPs for cancer therapy [9].

Various types of metal-containing NPs have been reported to cross the blood–brain barrier [10], suggesting that copper oxide NPs (CuO-NPs) have the potential to enter the brain and to affect properties and functions of brain cells. Indeed, peripheral application of CuO-NP to animals has been connected with cognitive alterations and oxidative stress in brain [11, 12]. On the cellular level, in vitro studies revealed that CuO-NPs are able to damage cells associated with the blood–brain barrier [13] and show a severe and concentration-dependent toxic potential to cultured primary brain astrocytes [7] and neuronal cells [14, 15].

Several studies have demonstrated that CuO-NPs in dispersion rapidly release copper ions [16–18]. These CuO-NP-derived copper ions are considered to strongly contribute to the cytotoxic potential of the NPs observed for cell cultures of peripheral origin [19–21] as well as for cultured glial cells [22]. However, the specific contribution of CuO-NPs in the observed glial cell toxicity after application of CuO-NP dispersions under conditions that eliminate the adverse consequences of the CuO-NP-derived contaminating copper

✉ Ralf Dringen
ralf.dringen@uni-bremen.de

[1] Center for Biomolecular Interactions Bremen, Faculty 2 (Biology/Chemistry), University of Bremen, PO. Box 330440, 28334 Bremen, Germany

[2] Center for Environmental Research and Sustainable Technology, Leobener Strasse, 28359 Bremen, Germany

[3] Fraunhofer Institute for Manufacturing Technology and Advanced Materials, Wiener Strasse 12, 28359 Bremen, Germany

ions has to our knowledge not been reported. At least for an epithelial cell line, the elimination of contaminating copper ions by synthetic chelating beads has prevented the cytotoxicity observed after exposure of the cells to fast-dissolving CuO-NPs [20, 23].

We have recently demonstrated that C6 glioma cells efficiently accumulate dimercaptosuccinate (DMSA)-coated CuO-NPs in a time-, concentration- and temperature-dependent manner which was accompanied by severe toxicity [22]. However, for the conditions used in this study it was concluded that contaminating copper ions which had been extracellularly released from the CuO-NPs, strongly contribute to the toxicity observed after application of a CuO-NP dispersion to C6 cells [22]. This initial study was now extended in order to study the real contribution of CuO-NPs in the cellular copper accumulation and copper-induced toxicity in glial cells after applications of CuO-NP dispersions. To do so, we have incubated C6 glioma cells as well as cultured primary astrocytes with CuO-NPs or $CuCl_2$ in the absence or the presence of a low concentration of the membrane-impermeable copper chelator bathocuproine disulfonate (BCS) [24], to chelate contaminating extracellular copper ions. Our new data clearly demonstrate that the presence of a low concentration of BCS did not affect copper accumulation and copper-induced toxicity after exposure of glial cells to CuO-NPs, but strongly lowered copper uptake and copper-mediated toxicity during exposure of the cells to ionic copper. This confirms that intact CuO-NPs are taken up into glial cells and mediate the specific toxic potential of such NPs.

Materials and Methods

Materials

Copper nitrate trihydrate and 4-(2-hydroxyethyl)-1-piperazineethanesufonic acid (HEPES) were obtained from Roth (Karlsruhe, Germany). Copper chloride, magnesium chloride hexahydrate, potassium chloride and sodium bicarbonate were purchased from Riedel-de Haën (Seelze, Germany). Bovine serum albumin (BSA), NADH and sodium ascorbate were purchased from Applichem (Darmstadt, Germany). Fetal calf serum (FCS), trypsin solution and penicillin/streptomycin solution were obtained from Biochrom (Berlin, Germany) and Dulbecco's modified Eagle's medium (DMEM) from Gibco (Karlsruhe, Germany). Folin–Ciocalteau's reagent, D-glucose, di-sodium hydrogen phosphate, sodium pyruvate, calcium chloride dihydrate, nitric acid and dipotassium phosphate trihydrate were purchased from Merck (Darmstadt, Germany). 2,3-Dimercaptosuccinic acid (DMSA), sodium chloride, bathocuproine disulfonic acid disodium salt (BCS) and bisbenzimide Hoechst 33342 (H33342) were from Sigma-Aldrich (Steinheim, Germany). Sodium hydroxide, Triton X-100, propidium iodide and potassium phosphate were obtained from Fluka (Buchs, Switzerland). 24-well cell culture plates and 96-well microtiter plates were obtained from Sarstedt (Nümbrecht, Germany).

Synthesis of DMSA-Coated Copper Oxide Nanoparticles

DMSA-coated CuO-NPs [7, 22] have the disadvantage to disintegrate and agglomerate rapidly after synthesis which requires continuous synthesis of fresh CuO-NPs for cell culture studies. To improve the colloidal stability of the NPs, CuO-NPs were synthesized and coated for the current study by a modification of a published method [7, 22]. Briefly, 20 mM copper nitrate solution in H_2O (50 mL) was heated under vigorous stirring to 75 °C, before addition of 1 M NaOH (2.1 mL) to induce NP formation. After 10 min of stirring at 75 °C, 50 mL of a pre-warmed (60 °C) 5 mM DMSA solution in H_2O was added to the CuO-NP dispersion and the heating was switched off. After 15 min of additional stirring, 50 mL of pre-warmed (60 °C) 10 mM DMSA solution in H_2O was added as a second coating step. The dispersion was then allowed to stir for another 15 min (60 °C) before centrifugation for 10 min at 1500 *g*. The supernatant was discarded and the NP pellet was washed with water. The remaining washing solution was removed by a subsequent centrifugation step. The resulting CuO-NPs were dispersed in 5 mM NaOH and sonicated thrice for 5 min at 50 W with a Branson B-12 sonifier (Danbury, Connecticut, USA). Lastly, the CuO-NP dispersion was filtered through a 0.2 µm filter before determination of the total copper content by atomic absorption spectroscopy (AAS). Copper concentrations of CuO-NP dispersions are given as concentration of total copper present in the dispersion, and not as particle concentration.

Characterization of Copper Oxide Nanoparticles

The hydrodynamic diameter and the zeta potential of the synthesized CuO-NPs in water and physiological incubation buffer were determined by dynamic (DLS) and electrophoretic (ELS) light scattering in a Beckman Coulter (Krefeld, Germany) Delsa Nano C Particle Analyzer at 25 °C, as previously described [7]. Samples for transmission electron microscopy (TEM) were prepared by dropping 10 µL of 1 mM CuO-NPs onto carbon-coated gold grids at room temperature. Subsequently, the grid was washed with 10 µL pure water twice before letting it air-dry. The TEM imaging was carried out by a FEI Tecnai F20 S-TWIN (Hillsboro, Oregon, USA) operated at 200 kV using a GATAN GIF2001 SSC-CCD camera (Pleasanton, California, USA).

TEM analysis of air-dried metal oxide NP dispersions is considered a challenge [25, 26]. Consistent with a previous report [7], it was especially difficult to obtain high quality images of the nanoparticulate structure of DMSA-coated CuO-NPs for the air-dried dispersions of these NPs in protein- and salt-containing solutions. Therefore, also high resolution TEM images were recorded which show the presence of 5 nm crystallite structures of the investigated CuO-NPs. Energy dispersive X-ray spectroscopy (EDX) for elemental analysis of the CuO-NP dispersion was carried out in the scanning mode of the microscope (STEM) with an EDAX r-TEM–EDX-detector with an energy resolution of 136 eV measured at Mn-Kα, as previously described [7].

Cell Cultures

The C6 glioma cell line has a male karyotype and is derived from a tumor induced in Wistar rats by exposure to *N*,*N*′-nitroso-methyl-urea [27]. The C6 glioma cell line was kindly provided by Dr. Frank Dietz (University of Bremen). Immunocytochemical staining of the C6 cells used in this study revealed that they express the astrocytic marker protein glial fibrillary acidic protein (GFAP) as described recently [28]. The C6 glioma cell-line was cultured as recently described in detail [22]. 80% confluent cell-cultures were harvested and cells were seeded in 1 mL culture medium at a density of 200,000 viable cells per mL into wells of 24-well culture plates, 24 h prior to beginning of experimental incubations.

Astrocyte-rich primary cultures were prepared from the brains of new-born Wistar rats from a litter without separating or counting male and female pups and cultured as previously described [29]. The experiments presented here were performed on confluent cultures of an age of 14–35 days. Immunocytochemical staining of these cultures revealed that they consisted predominantly of astrocytes and that only minor amounts of other glial cells types are present in these cultures [29].

Experimental Incubations with Copper

The cells were washed twice with 1 mL of pre-warmed (37 °C) incubation buffer (IB-BSA; 20 mM HEPES, 145 mM NaCl, 5 mM D-glucose, 1.8 mM $CaCl_2$, 5.4 mM KCl, 1 mM $MgCl_2$, 0.5 mg/mL BSA, pH 7.4) in the wells of a 24-well cell-culture plate. Subsequently, the cells were incubated for the indicated time periods at 37 °C in the humidified atmosphere of an incubator with 200 µL IB-BSA supplemented with CuO-NPs or $CuCl_2$ (ionic copper) in the concentrations given in the legends of the figures. To study the effects of the copper chelator BCS, the cells were exposed to CuO-NPs or $CuCl_2$ (control for ionic copper) in IB-BSA that contained BCS in a concentration amounting to 20% (unless stated otherwise) of the total concentration of copper applied (IB-BSA-BCS). Following the incubations, the cells were washed twice with 1 mL pre-warmed (37 °C) IB-BSA to subsequently determine cell viability. Alternatively, cultures were washed with 1 mL ice-cold (4 °C) phosphate buffered saline (PBS; 10 mM potassium phosphate buffer containing 150 mM sodium chloride, pH 7.4) and dry cells were stored at -20 °C until subsequent quantification of copper and protein contents.

Cellular Copper and Protein Quantification

The frozen dry cells in the wells of 24-well plates were lysed in 400 µL of 50 mM NaOH in water for 2 h and this cell lysate was used to determine protein and copper contents. The cellular copper content was determined for 100 µL of the cell lysate that had been ashed as described previously [7]. Copper quantification was done by the graphite furnace AAS using a Varian AA-240Z spectrophotometer (Darmstadt, Germany) and a Varian GTA-120 graphite tube atomizer as described earlier [7]. The protein content of the cultures was quantified according to the Lowry method [30], using BSA as standard protein. The cellular copper content of a sample was normalized to the protein content of the respective sample to obtain the specific cellular copper content.

Viability Assays

Cell viability was determined by quantification of the activity of the cellular lactate dehydrogenase (LDH) [29]. For this purpose, the cells were lysed after a given treatment with 1% (v/v) Triton X-100 in 200 µL IB-BSA for 30 min at 4 °C and 10 µL of this lysate was used for the determination of the cellular LDH activity. Impaired membrane integrity was also visualized by staining the cultures with the membrane impermeable fluorescent dye PI as described earlier [7, 29]. In such experiments, the membrane permeable dye Hoechst H33342 was applied to visualize all cell nuclei present. Images of the stained cultures were taken on the Eclipse TE2000-U fluorescent microscope using the appropriate filter settings: PI (λ_{ex}: 510–560 nm; λ_{em}: 590 nm; dichromatic mirror: 505 nm) and H33342 (λ_{ex}: 330–380 nm; λ_{em}: 435–485 nm; dichromatic mirror: 400 nm).

Quantification of Ionic Copper Liberated from Copper Oxide Nanoparticles

The ionic copper liberated from CuO-NPs after application of a given concentration of BCS was quantified by determining the absorbance of the copper-BCS complex formed at 484 nm [31, 32]. Briefly, 1 mM CuO-NPs were incubated without or with BCS in concentrations of up to 4 mM in

IB-BSA at room temperature. After 1 h, 20 µL of the samples were diluted with 180 µL 20 mM Tris/HCl (containing 200 mM NaCl, pH 7.2) containing no or 1 mM of the reducing agent ascorbate in wells of a microtiter plate. Subsequently, the absorbance of the generated Cu-BCS complex was determined at 484 nm in a MultiSkan Sky microtiter plate photometer (Life Technologies, Darmstadt, Germany) and was compared with the absorbances of copper standards (0–1.5 mM $CuCl_2$ in IB-BSA) that had been generated by mixing 20 µL standards with 180 µL detection reagent (1 mM BCS and 1 mM ascorbate in 20 mM Tris/HCl with 200 mM NaCl, pH 7.2).

Presentation of Data

The quantitative data shown in the figures and the table represent means ± standard deviations (SD) of values derived from *n* independent experiments that were performed on different cell passages or independently prepared primary astrocyte cultures. Cell images showing cytochemical staining are from a representative experiment that was reproduced at least once in an independent experiment with similar outcome. Statistical analysis between multiple groups of data was performed by ANOVA followed by the Bonferroni's post hoc test, whereas statistical analysis between two sets of data was performed by the paired Student's *t*-test or unpaired Student's *t*-test (Welch corrected), using the program GraphPad InStat. Values of $p > 0.05$ were considered not significant.

Results

Synthesis and Characterization of DMSA-Coated CuO-NPs

An improved wet chemical precipitation method was used to synthesize DMSA-coated CuO-NPs which contained a two-step DMSA coating procedure. Characterization of the newly synthesized CuO-NPs dispersions via TEM analysis revealed primary crystalline particles with a diameter of around 5 nm in the dispersants water (Fig. 1a, b), IB-BSA (Fig. 1d, e) or IB-BSA-BCS (Fig. 1g, h). For the CuO-NP dispersion in water, specific elemental peaks for the presence of copper (Cu), oxygen (O) and sulphur (S) (Fig. 1c) were identified via EDX analysis. Peaks present for the elements carbon (C) and gold (Au) indicate elemental composition of the TEM grid (Fig. 1c). EDX analysis of CuO-NPs in IB-BSA (Fig. 1f) and IB-BSA-BCS (Fig. 1i) revealed almost identical elemental peaks as those observed for water-dispersed CuO-NPs. Thus, the addition of BCS to the physiological media did not alter the size or elemental composition of the CuO-NPs.

Characterization by DLS and ELS of CuO-NPs that had been dispersed in water revealed an average hydrodynamic diameter of the NPs of 124 ± 11 nm and a zeta (ζ) potential of − 63.6 ± 7.9 mV. CuO-NPs dispersed in IB-BSA had a slightly increased hydrodynamic diameter of 191 ± 33 nm, while the ζ-potential became with − 13.1 ± 0.3 mV significantly more positive (Table 1). The presence of the copper chelator BCS in IB-BSA did not significantly ($p > 0.05$) alter the physicochemical parameters of dispersed CuO-NPs compared to dispersions in BCS-free IB-BSA (Table 1). The almost identical polydispersity indices of approximately 0.2 of the investigated CuO-NP dispersions demonstrated a homogenous size distribution of the particle population which was not altered by the absence or the presence of BCS (Table 1).

The second DMSA-coating improved the colloidal stability of the CuO-NP dispersion in water as demonstrated by the absence of any obvious precipitation for up to 30 d after synthesis (compared to around 14 days for CuO-NPs synthesized by the previously used method [7, 22]) and by the absence of any significant alteration in the average hydrodynamic diameter or the zeta potential of the dispersed CuO-NPs during storage for up to 30 d (data not shown).

CuO-NP-Induced Copper Accumulation and Toxicity in C6 Glioma Cells

To study the uptake and potential toxicity of the synthesized DMSA-coated CuO-NPs, C6 glioma cells were incubated in the absence or the presence of CuO-NPs for up to 5 h (Fig. 2). Untreated C6 cells had a specific cellular copper content of 0.27 ± 0.29 nmol/mg protein ($n = 12$) and this value did not change during an incubation in the absence of CuO-NPs for up to 5 h (Fig. 2a). In contrast, exposure of C6 cells to 100 µM, 500 µM and 1000 µM CuO-NPs increased the specific cellular copper content within 3 h to values of around 50, 140 and 200 nmol/mg protein, respectively (Fig. 2a). During the incubation in the absence or in the presence of 100 µM CuO-NPs, the cell viability was not compromised as indicated by the absence of any significant loss in cellular LDH activity during the incubation (Fig. 2b). In contrast, strong cytotoxicity was observed for cells that had been exposed to 500 µM or 1000 µM CuO-NPs as demonstrated by the severe loss in cellular LDH activity during the initial 3 h of incubation (Fig. 2b). Correlation of the specific cellular copper content to the cellular LDH activity revealed that a loss in cell viability of C6 cells was only observed for incubations that had led upon treatment with CuO-NPs to specific cellular copper contents exceeding 50 nmol/mg protein (Fig. 2c).

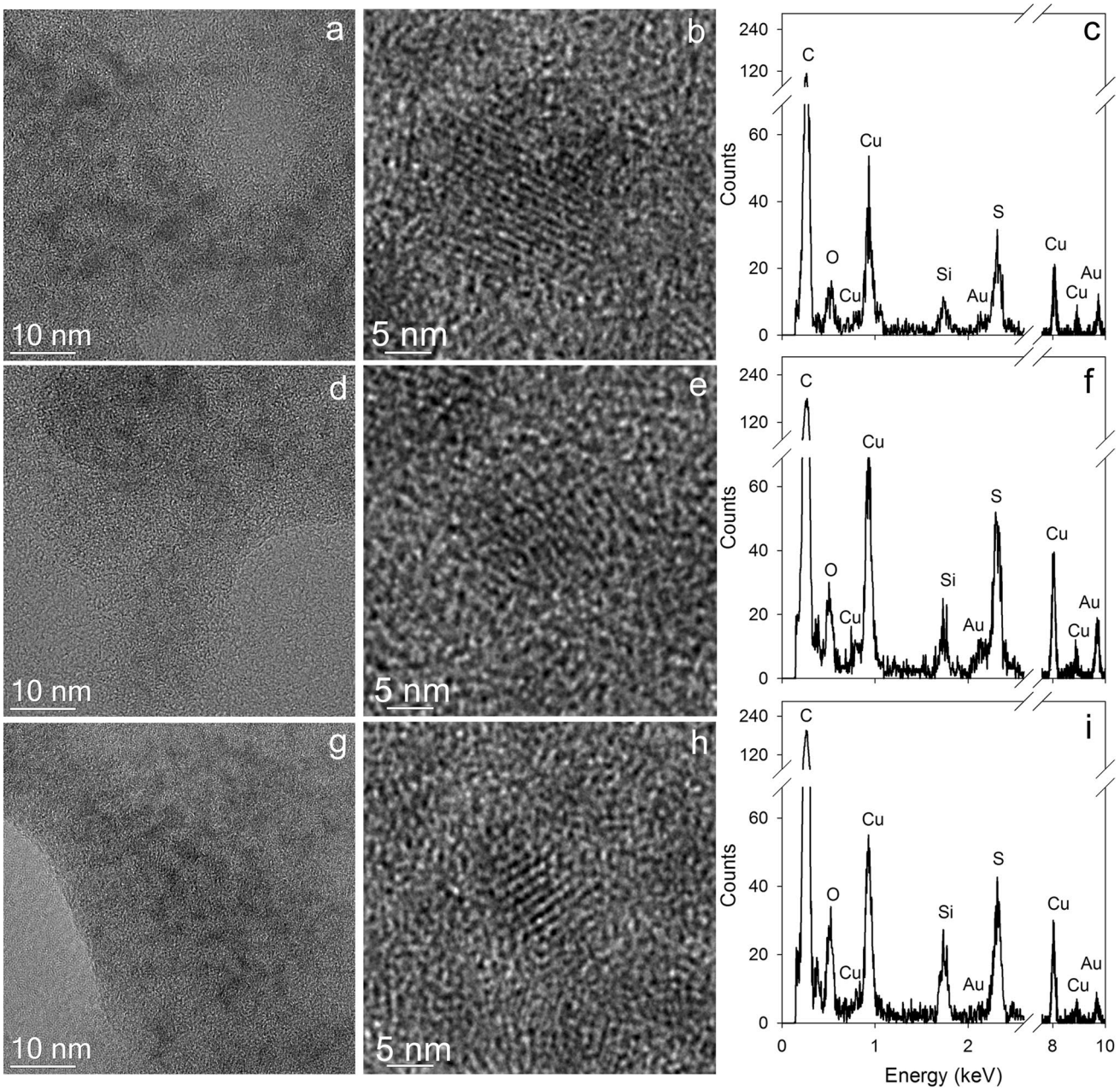

Fig. 1 Characterization of CuO-NPs. DMSA-coated CuO-NPs that had been dispersed in a concentration of 1 mM in water (**a**–**c**), in IB-BSA (**d**–**f**) or in IB-BSA-BCS (**g**–**i**) were dropped onto carbon-coated gold grids and visualized by transmission electron microscopy. Electron dense material was observed for all three preparations (**a**, **d**, **g**). Higher magnifications revealed the presence of primary crystalline particles of a diameter of around 5 nm (**b**, **e**, **h**). Analysis of the elemental composition of the electron dense material by energy-dispersive X-ray spectroscopy revealed the presence of copper, oxygen as well as of the sulfur derived from the DMSA coat (**c**, **f**, **i**)

Effects of 20% BCS on the Viability and Copper Content of C6 Cells that had been Treated with CuO-NPs or Ionic Copper

Contaminating copper ions in CuO-NPs dispersions have been addressed to substantially contribute to the copper accumulation and to the copper-induced toxicity of cells exposed to CuO-NPs [5, 22, 23, 33]. Analysis of the content of ionic copper in the CuO-NP dispersion stored in water for up to 30 d after synthesis revealed that up to 10% of the total copper in the dispersion had been released from the NPs as ionic copper (data not shown). In order to extracellularly chelate the ionic copper in the CuO-NP dispersion, the membrane-impermeable copper chelator BCS which binds copper ions in a 2 to 1 stoichiometry [24, 34] was applied in a final concentration that represented 20% of the applied

Table 1 Characterization of CuO-NPs

	Hydrodynamic diameter (nm)	*n*	Polydispersity index	*n*	Zeta potential (mV)	*n*
H_2O	124 ± 11	20	0.205 ± 0.02	20	− 63.6 ± 7.9	8
IB-BSA	191 ± 33***	4	0.225 ± 0.03	4	− 13.1 ± 0.3***	4
IB-BSA-BCS	168 ± 19***	4	0.215 ± 0.01	4	− 12.9 ± 1.4***	4

DMSA-coated CuO-NPs were synthesized and the hydrodynamic diameter, polydispersity index and zeta potential of 1 mM dispersions in water, in IB-BSA or in IB-BSA-BCS were determined. Data were obtained from particles derived from *n* independent syntheses. Asterisks indicate the significance of differences (ANOVA) to the values determined for CuO-NPs dispersed in water (***p < 0.001)

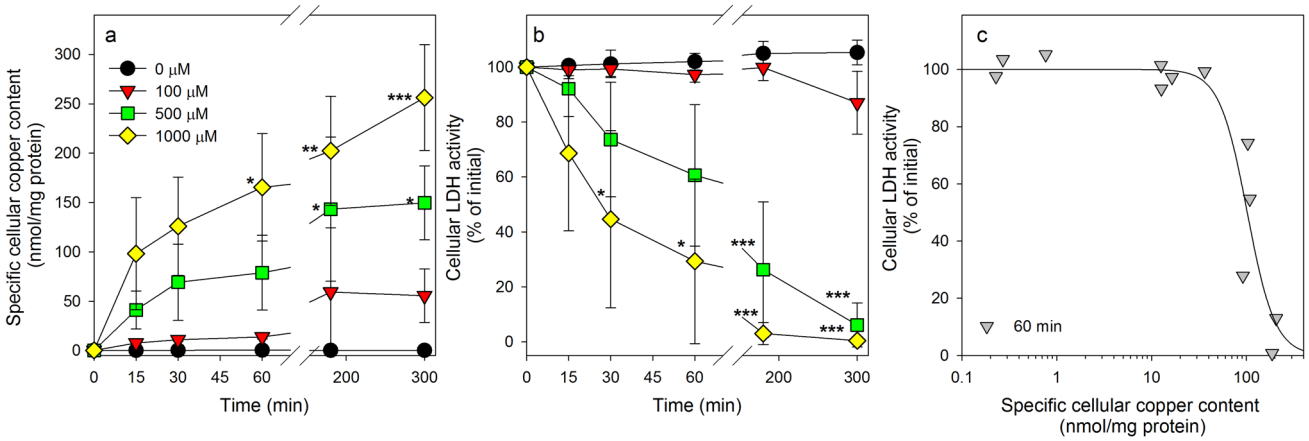

Fig. 2 Time- and concentration-dependent consequences of an exposure of C6 glioma cells to CuO-NPs. The cells were incubated without or with the indicated concentrations of CuO-NPs in IB-BSA for up to 5 h at 37 °C (**a**, **b**) and subsequently the cellular copper content (**a**) and the cellular LDH activity (**b**) were determined. Panel **c** shows the correlation between the specific cellular copper contents determined after exposure to CuO-NPs for 60 min and the respective values for the cellular LDH activity. The data shown represent means ± standard deviation of the individual values obtained in the 3 independent experiments performed. The 100% cellular LDH activity values in panel **b** correspond to 2438 ± 377 nmol/(min × mg protein). In panels **a** and **b**, asterisks indicate the significance of differences of data (ANOVA) compared to the values obtained for control cells that had been incubated in the absence of NPs (*p < 0.05, **p < 0.01, ***p < 0.001)

copper concentration (Fig. 3). To also directly test for the adverse effects of ionic copper under the conditions used for the cell experiments $CuCl_2$ was applied as alternative copper source.

In the absence of BCS, a concentration-dependent decline in cell viability was observed after exposure of C6 cells to CuO-NPs (Fig. 3a) or ionic copper (Fig. 3d) for 1 h, which became significant compared to control cells (incubated in the absence of copper) for incubations with CuO-NPs or $CuCl_2$ in concentrations of 500 µM (Fig. 3a, d). A corresponding concentration-dependent increase in the specific cellular copper content was also observed after incubations with CuO-NPs (Fig. 3b) or $CuCl_2$ (Fig. 3e). The specific cellular copper content of C6 cells after exposure for 1 h to CuO-NPs in concentrations of 500–1000 µM was increased to values of 120 to 150 nmol/mg protein (Fig. 3b), while C6 cells contained between 250 and 400 nmol copper/mg protein after incubations with the respective concentrations of ionic copper (Fig. 3e). Half-maximal loss in cellular LDH activity was observed for cells that had accumulated copper to values of 103 ± 43 nmol/mg and 183 ± 100 nmol/mg after exposure to CuO-NPs and ionic copper, respectively (Fig. 3c, f).

Presence of 20% BCS during the incubation did not affect the concentration-dependent decline in cellular LDH activity observed for BCS-free incubations of C6 cells with CuO-NPs (Fig. 3a), the corresponding gradual increase in cellular copper content (Fig. 3b) nor the specific cellular copper content that correlated to a 50% loss in cellular LDH activity (100 ± 24 nmol/mg) (Fig. 3c). In contrast, the severe toxicity and the substantial copper accumulation observed for C6 cells that had been incubated with ionic copper was strongly lowered for incubations in the presence of BCS (Fig. 3d, e) and a half-maximal loss in cellular LDH activity was only detectable for BCS-treated cells that contained around 220 nmol copper/mg protein (Fig. 3f).

The loss in cellular LDH activity as indicator for cell toxicity after an exposure of C6 cells with 500 µM CuO-NPs

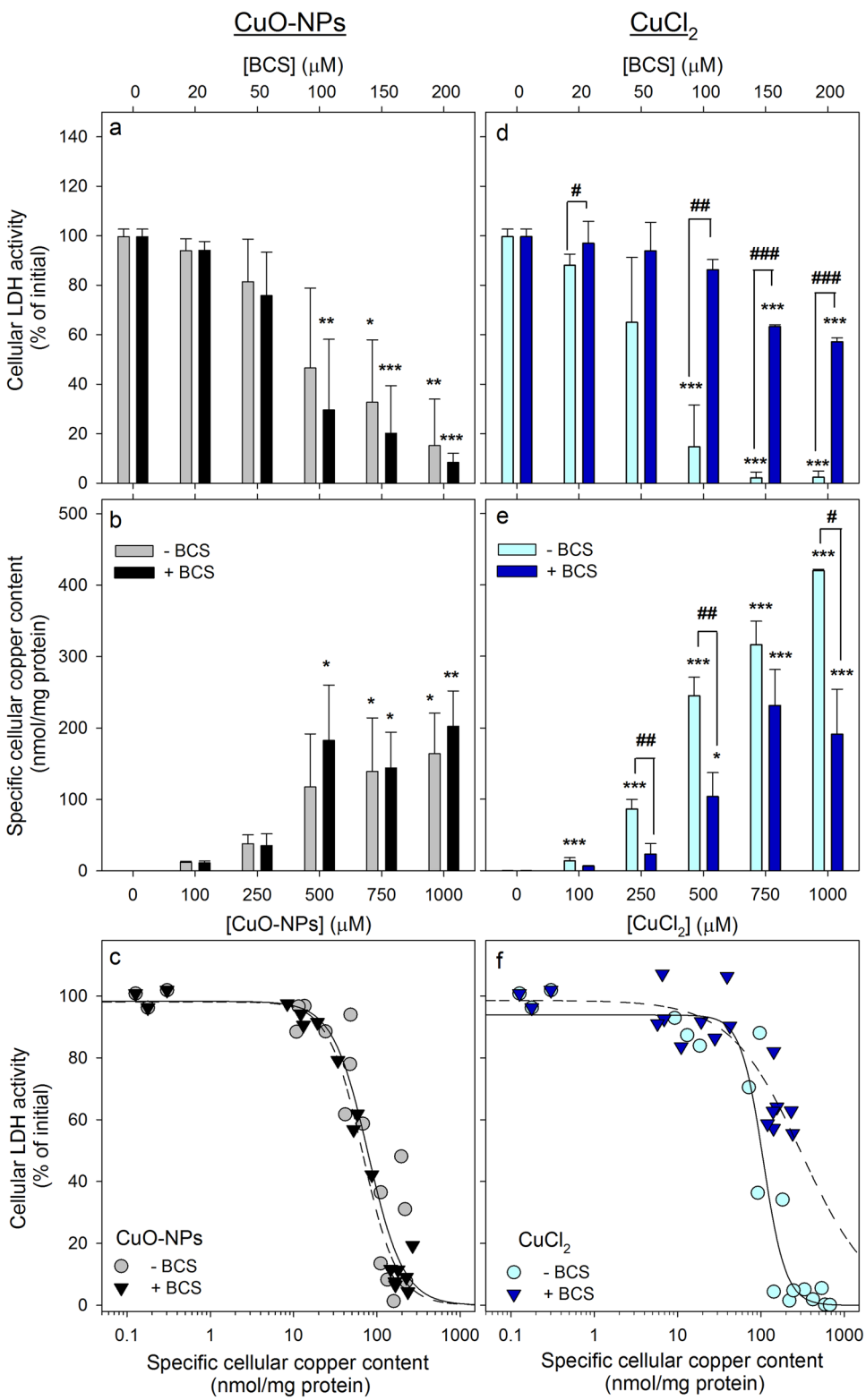

Fig. 3 Toxicity and copper accumulation after exposure of C6 glioma cells to CuO-NPs and $CuCl_2$ in the absence or the presence of BCS. The cells were incubated for 1 h at 37 °C in IB-BSA containing the indicated concentrations of CuO-NPs (**a**, **b**) or $CuCl_2$ (**d**, **e**) in the absence or the presence of BCS in a concentration that accounted for 20% of the molar concentration of copper applied. Subsequently, the cellular LDH activity (**a**, **d**) and the cellular copper contents (**b**, **e**) were determined. Panels **c** and **f** show the correlation between the specific cellular copper contents determined after exposure to CuO-NPs (**c**) or $CuCl_2$ (**f**) and the respective values for the cellular LDH activity. The 100% cellular LDH activity values in panels **a** and **d** correspond to 2527 ± 357 nmol/(min × mg protein). The data shown in panels **a**, **b**, **d**, and **e** represent means ± SD of values obtained in three independent experiments. Panels **c** and **f** show the correlation for the individual data obtained in the three experiments performed. Asterisks indicate in panels **a**, **b**, **d** and **e**) the significance of differences of data (ANOVA, *$p < 0.05$, **$p < 0.01$, ***$p < 0.001$) compared to control cells that had been incubated in the absence of CuO-NPs and $CuCl_2$. Hashes indicate the significance of differences (paired *t*-test) of data obtained for cells that had been treated without or with BCS ($^{\#}p < 0.05$, $^{\#\#}p < 0.01$, $^{\#\#\#}p < 0.001$)

or ionic copper for 1 h was validated by investigating the membrane integrity of cells by PI staining. In cultures that had been incubated without any copper (without or with BCS), PI-positive cells were not observed (Fig. 4a, g), while substantial numbers of PI-positive cells were detectable after incubations with CuO-NPs (Fig. 4b, e) or ionic copper (Fig. 4c, f). The high number of PI-positive cells in C6 cultures that had been incubated with CuO-NPs in BCS-free

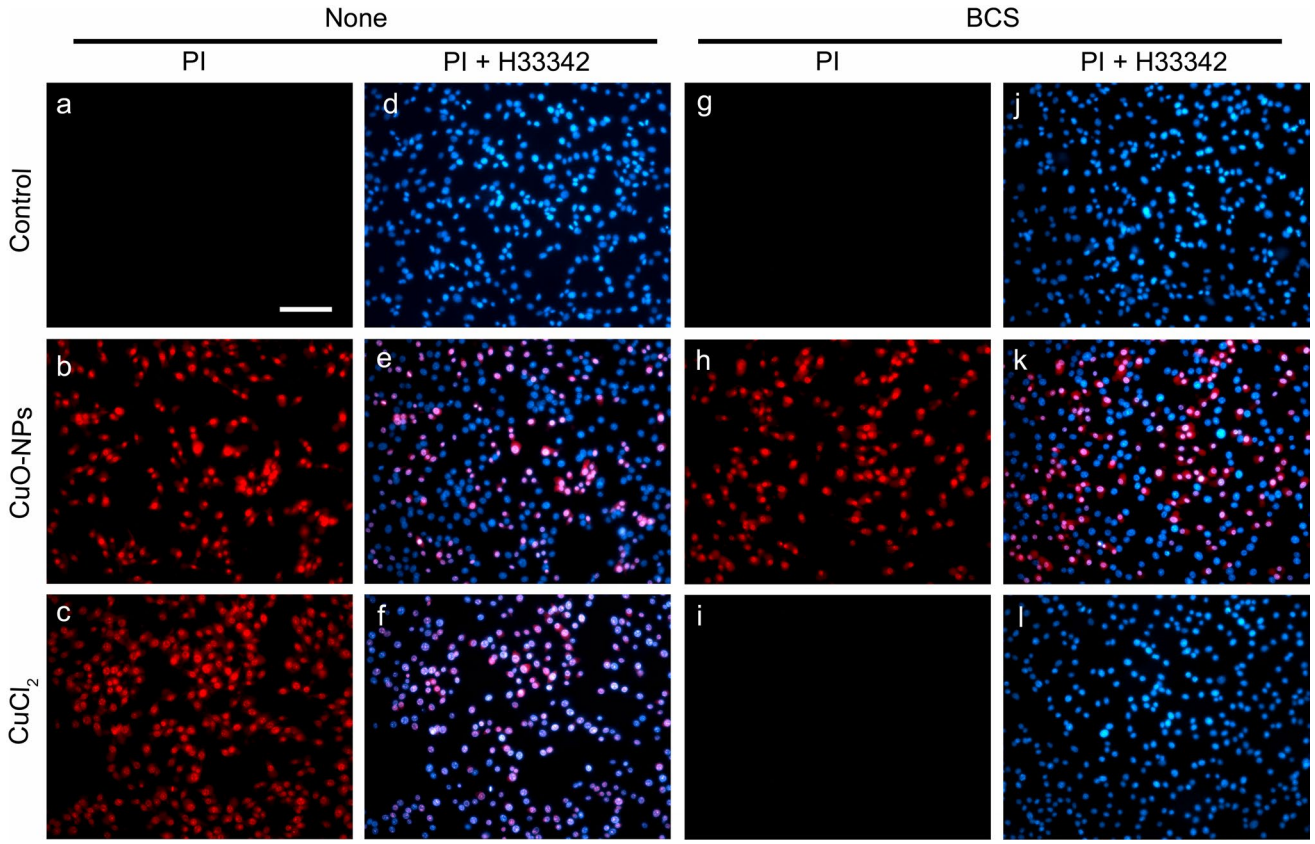

Fig. 4 Membrane integrity of C6 glioma cells after treatment with CuO-NPs or $CuCl_2$. Cells were incubated without (control) or with 500 µM CuO-NPs or $CuCl_2$ in IB-BSA for 1 h at 37 °C in the absence (none) (**a–f**) or the presence (**g–l**) of 100 µM BCS. Subsequently, the cultures were stained for membrane integrity by application of PI and the cell nuclei were visualized with H33342. Shown are representative images of the PI stainings in red (**a–c**, **g–i**) and the merged images of the PI (red) and the H33342 (blue) stainings (**d–f**, **j–l**). The scale bar in panel **d** represents 50 µm and applies to all panels (Color figure online)

medium (Fig. 4b, e) was not lowered by the presence of 20% BCS (Fig. 4h, k), while PI-staining was not observed in cultures that had been co-incubated with ionic copper and BCS (Fig. 4i, l).

Temperature-Dependent Copper Accumulation in Copper-Treated C6 Glioma Cells

To evaluate the effect of temperature on the copper accumulation and toxicity of copper-treated C6 glioma cells, the cells were incubated for 1 h at 37 °C or 4 °C with 500 µM CuO-NPs or $CuCl_2$ in the absence or presence of 100 µM BCS (Fig. 5). Treatment of cells with CuO-NPs and $CuCl_2$ in the absence of BCS at 37 °C, lowered the cellular LDH activity to 50% and 15%, respectively, of the initial cellular LDH activity (Fig. 5a), while the cells had accumulated large amounts of copper yielding in specific cellular copper contents of 120 nmol/mg (CuO-NPs) and 220 nmol/mg ($CuCl_2$) (Fig. 5c). Presence of 20% BCS during the 37 °C incubation with CuO-NPs neither affected the loss in cellular LDH activity (Fig. 5a, b), nor the cellular copper accumulation significantly (Fig. 5c, d). In contrast, incubation of C6 cells at 37 °C with $CuCl_2$ in the presence of 20% BCS prevented the loss in cellular LDH activity (Fig. 5a, b) and lowered the cellular copper accumulation significantly by around 40% (Fig. 5d) compared to cells that had been incubated in the absence of BCS (Fig. 5c). Respective incubations at a temperature of 4 °C for all conditions applied completely prevented the loss in cellular LDH activity (Fig. 5a, b) and the extensive cellular copper accumulation (Fig. 5c, d).

Concentration Dependent-Effects of the Copper Chelator BCS in C6 Glioma Cells

The application of BCS in a 20% molar ratio to copper protected C6 cells against the toxicity observed during incubation with copper ions but not against CuO-NP-induced toxicity. In order to test for the potential of higher concentrations of BCS to affect copper accumulation and copper-induced toxicity of copper-treated C6 cells, the cells were incubated with 1 mM of CuO-NPs or $CuCl_2$ in the absence or the presence of BCS in concentrations of up to 4 mM for 1 h at

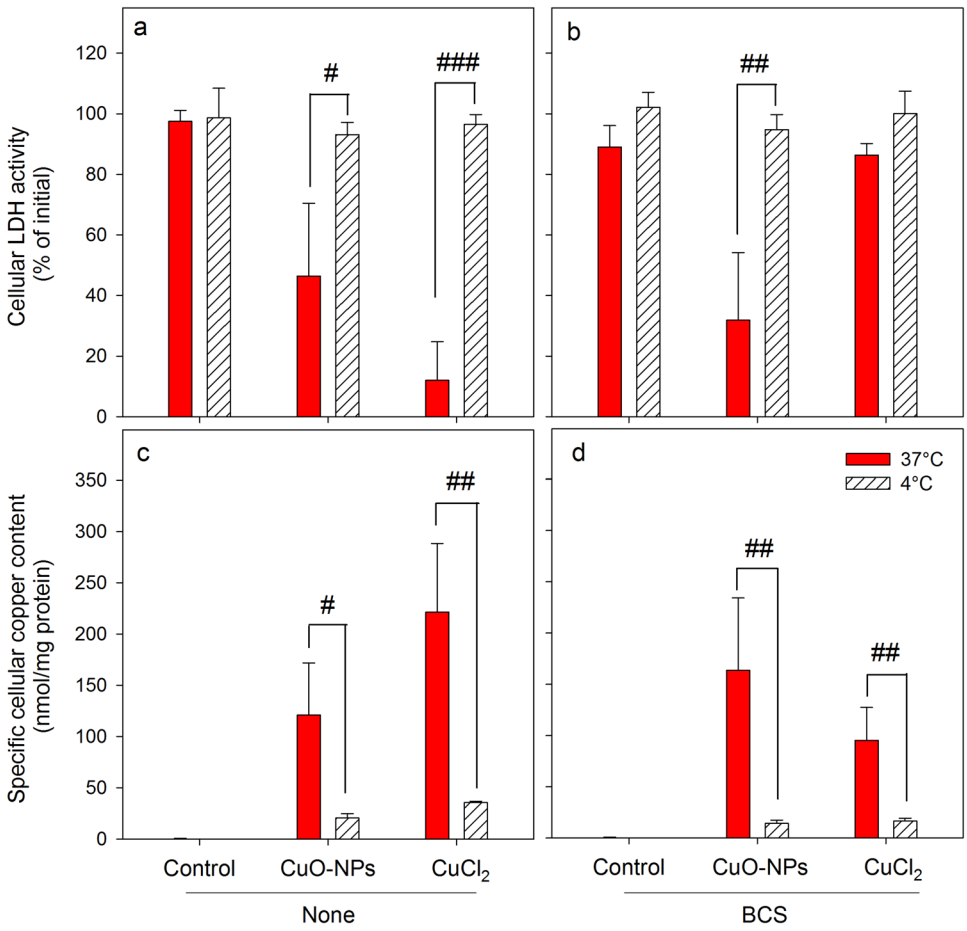

Fig. 5 Temperature-dependent copper accumulation and toxicity after exposure of C6 glioma cells to CuO-NPs or $CuCl_2$. The cells were incubated without (control) or with 500 µM CuO-NPs or $CuCl_2$ in IB-BSA for 1 h at 37 °C or 4 °C in the absence or the presence of 100 µM BCS. Subsequently, the cellular LDH activity (**a**, **b**) and the specific cellular copper contents (**c**, **d**) were determined. The 100% cellular LDH activity values in panel a correspond to 2234 ± 518 (37 °C) and 1773 ± 34 nmol/(min × mg protein) (4 °C). The data shown represent means ± SD of values obtained in five (37 °C) or three (4 °C) independent experiments. Hashes indicate the significance of differences of data (unpaired *t*-test) obtained for cultures that had been incubated at 37 °C or 4 °C ($^{\#}p < 0.05$, $^{\#\#}p < 0.01$, $^{\#\#\#}p < 0.001$)

37 °C and the cellular LDH activity and the cellular copper content were determined (Fig. 6). Control incubations of cells without copper revealed that during this incubation the cultures did not suffer from any loss in cellular LDH activity and contained very low cellular copper contents (Fig. 6a, b). However, after incubation with 1 mM CuO-NPs or ionic copper in the absence of BCS a severe loss in cellular LDH activity (Fig. 6a, c) and a strong copper accumulation to specific cellular copper contents of up to 300 nmol/mg protein were observed (Fig. 6b). The presence of BCS in concentrations of up to 1 mM for 1 h did not alter the CuO-NP-induced toxicity (Fig. 6a) and only slightly altered the specific cellular copper content (Fig. 6b), while higher concentrations of BCS (2 or 4 mM) completely prevented the CuO-NP-induced loss in cell viability as well as the cellular copper accumulation. For cells exposed to 1 mM ionic copper, the presence of 0.1 mM BCS was already sufficient to prevent the toxicity in C6 cells (Fig. 6a, c) and this was accompanied by a gradual loss in cellular copper accumulation with increasing concentrations of BCS (Fig. 6a, b). A half-maximal loss in cellular LDH activity was only detectable for CuO-NP-treated cells that contained around 122 ± 25 nmol copper/mg protein, while for $CuCl_2$-treated cells under the same conditions a specific copper content of 195 ± 61 nmol/mg protein was accompanied with half-maximal toxicity (Fig. 6c).

Quantification of the concentration of copper ions released from 1 mM CuO-NPs by given concentrations of BCS revealed that, the amount of copper ions detected as Cu-BCS complex was for low BCS concentrations almost proportional to the concentration of BCS applied and that BCS in concentrations of 0.2 mM, 0.5 mM and 1 mM had liberated around 6%, 17% and 43% of the copper applied as CuO-NPs (Fig. 7). In contrast after incubations of CuO-NPs with 2 mM and 4 mM BCS around 76% and 85% of the applied copper were detectable as copper-BCS complex (Fig. 7).

Adverse Effects of an Exposure of Astrocyte-Rich Primary Cultures to CuO-NPs or $CuCl_2$

To test whether the results obtained for CuO-NP-exposed C6 cells can be confirmed for primary astrocytes, cellular copper accumulation as well as cell viability were studied after incubation of primary astrocyte cultures for 1 h with 500 µM CuO-NPs or $CuCl_2$ in the absence or the presence of

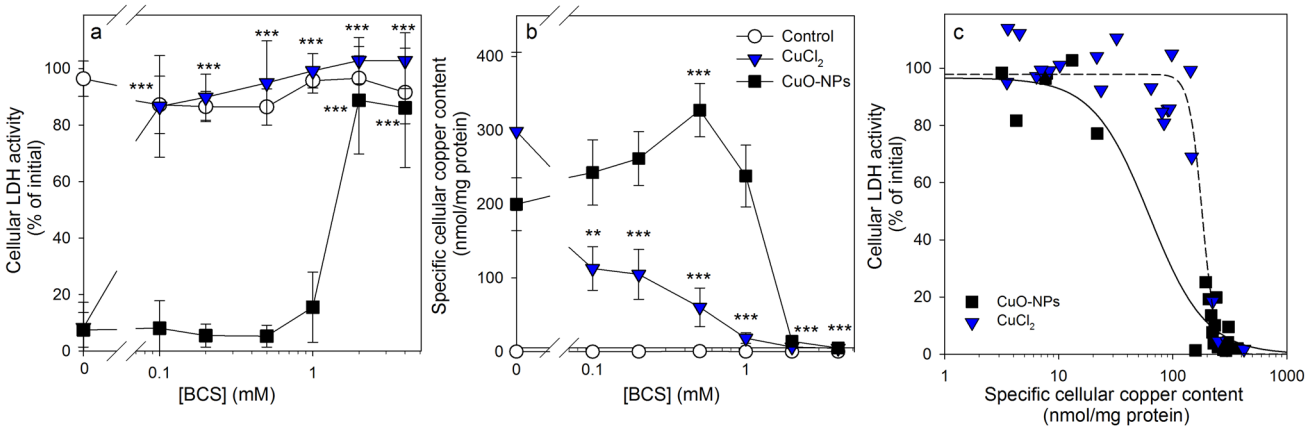

Fig. 6 Concentration-dependent modulation by BCS of the copper accumulation and viability of C6 glioma cells after exposure to CuO-NPs or $CuCl_2$. The cells were incubated without (control) or with 1 mM CuO-NPs or $CuCl_2$ for 1 h in IB-BSA at 37 °C in the absence or the presence of the indicated concentrations of BCS before the cellular LDH activity (**a**) and the specific cellular copper contents (**b**) were determined. Panel c shows the correlation between the specific cellular copper content and the respective values for cellular LDH activity obtained after exposure to CuO-NPs or $CuCl_2$ in the presence of indicated concentrations of BCS. The 100% cellular LDH activity value in panel a corresponds to 2478 ± 559 nmol/(min × mg protein). In panels **a** and **b**, the data shown represent mean ± SD of values obtained in 3 independent experiments and asterisks indicate the significance of differences of data (ANOVA) compared to the values obtained for incubations in the absence of BCS (**$p < 0.01$, ***$p < 0.001$). Panels **c** show the correlation for the individual data obtained in the three independently performed experiments

20% BCS (Fig. 8). For control incubations without copper, the cell viability of astrocyte cultures remained unaffected as demonstrated by the high cellular LDH activity (Fig. 8a)

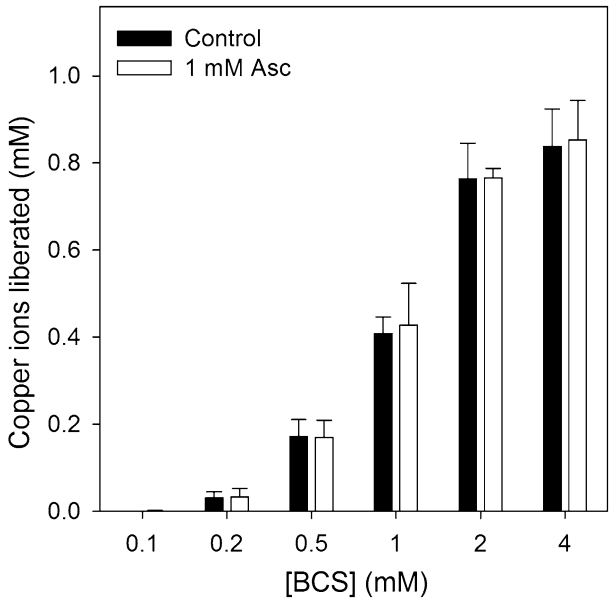

Fig. 7 Quantification of ionic copper liberated by BCS from CuO-NPs. 1 mM CuO-NPs were incubated in IB-BSA with BCS in the concentrations indicated for 1 h before the absorbance of the Cu-BCS complex was photometrically determined by comparison with the absorbance of standard concentrations of copper ions in the absence or the presence of 1 mM ascorbate. The data shown represent means ± SD of values obtained from 3 independent measurements

and the absence of PI-positive cells (Fig. 8c, i). In addition, copper accumulation was not detected for this condition (Fig. 8b). In contrast, substantial copper accumulation was observed to values of around 150 nmol/mg protein (Fig. 8b) as well as severe toxicity as indicated by a loss in cellular LDH activity (Fig. 8a) and by the appearance of PI-positive cells (Fig. 8d, j) for CuO-NP-treated astrocytes both in the absence (Fig. 8d, g) and in the presence (Fig. 8j, m) of 20% BCS. In contrast, presence of 20% BCS significantly lowered cellular copper accumulation in astrocytes that had been exposed to ionic copper (Fig. 8b) to values also observed for cells that had been incubated at 4 °C (data not shown), prevented copper-induced toxicity (Fig. 8a) and substantially lowered the appearance of PI-positive cells (Fig. 8k, n) compared to control cells that had been incubated with $CuCl_2$ in the absence of BCS (Fig. 8e, h).

Discussion

DMSA-coated CuO-NPs have previously been reported to cause toxicity in C6 glioma cells and primary astrocytes [23, 29]. As the stability of these CuO-NPs was limited and as copper ions were rapidly released from such particles [29] the initial coating procedure [23] was modified and improved by a second coating step with DMSA which also increased the colloidal stability of the NPs in water as demonstrated by an extended shelf-life. TEM analysis of the newly synthesized CuO-NPs revealed crystalline core particles with sizes of around 5 nm and EDX analysis showed the expected

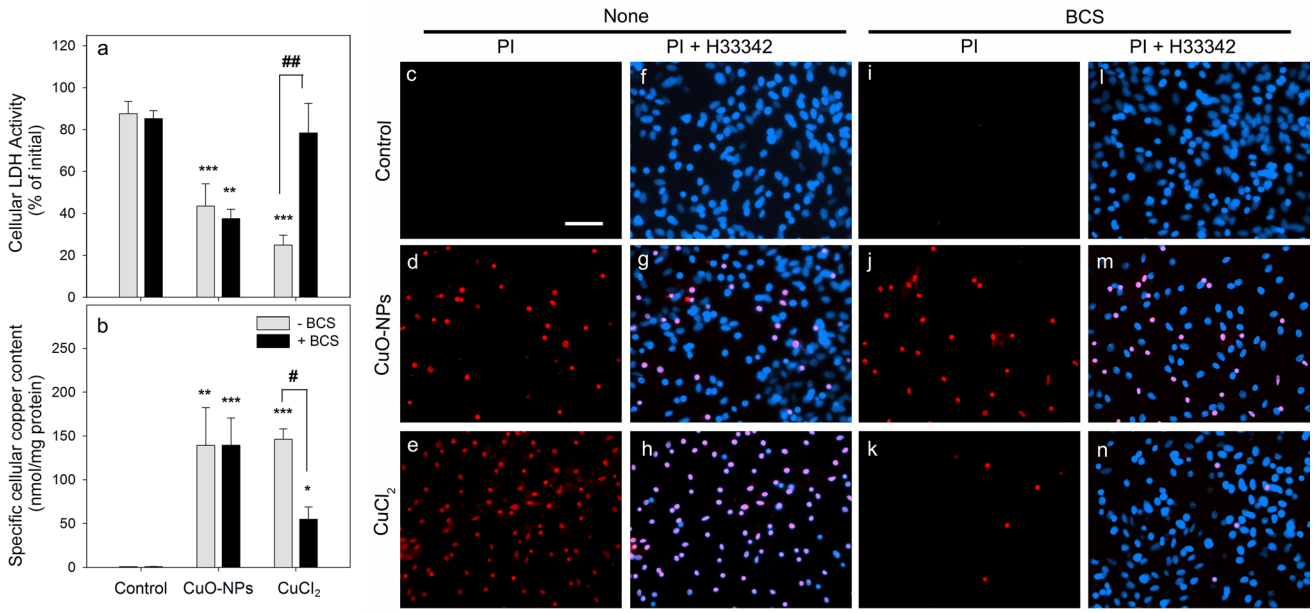

Fig. 8 Consequences of a treatment of primary astrocytes with CuO-NPs or $CuCl_2$. The cultures were incubated without (control) or with 500 µM CuO-NPs or $CuCl_2$ in IB-BSA for 1 h at 37 °C in the absence or the presence of 100 µM BCS. Subsequently, the cellular LDH activity (**a**) and the specific cellular copper content (**b**) were determined. In addition, the membrane integrity was monitored by PI and H33342 staining (**c**–**n**) and shown are representative images of the PI stainings in red (**c**–**e**, **i**–**k**) and the merged images of the PI (red) and the H33342 (blue) stainings (**f**–**h**, **l**–**n**). In panel **a**, the 100% cellular LDH activity values correlate to 1542 ± 207 nmol/(min × mg protein). The data shown in panels **a** and **b** are means ± SD of values obtained in 3 independent experiments performed on individually prepared astrocyte cultures. In panels **a** and **b** asterisks indicate the significance of differences of data (ANOVA) obtained for cells that had been treated in the absence (control) or the presence of copper (*$p < 0.05$, **$p < 0.01$, ***$p < 0.001$). Hashes indicate the significance of differences of data (paired *t*-test) obtained for cells that had been treated in the absence or the presence of BCS ($^{\#}p < 0.05$, $^{\#\#}p < 0.01$). The scale bar in panel **f** represents 50 µm and applies to panels **c**–**n** (Color figure online)

elemental composition [23], including the sulphur peak that confirms the presence of the DMSA coat. Physicochemical characterization for dispersions in water revealed an average hydrodynamic diameter of around 120 nm and a zeta potential of around –60 mV, data which are almost identical to those reported previously for DMSA-coated CuO-NPs [7] and confirmed the presence of agglomerates of the primary particles in dispersion as previously reported for copper-containing NPs [35, 36].

For cell experiments, the newly synthesized DMSA-coated CuO-NPs were applied in BSA-containing physiological buffer. The presence of BSA maintained the colloidal stability and prevented the agglomeration of NPs in physiological media, consistent with literature data [7, 37, 38]. The average hydrodynamic diameter of the dispersed NP aggregates increased slightly to around 190 nm and the zeta potential was more positive at around − 10 mV as previously reported for protein coated NPs [7, 39], demonstrating that the DMSA-coated CuO-NPs had been coated by an BSA layer. The additional BSA-coating of the DMSA-coated CuO-NPs did not affect the particle core size or the elemental composition of the NPs.

Application of the BSA- and DMSA-coated CuO-NPs to cultured glial cells caused a time-, concentration, and temperature-dependent accumulation of copper and copper-induced toxicity, as previously reported for such NPs [7, 22]. Impairment of C6 cell viability was only observed if the specific cellular copper content of the C6 cells had exceeded 50 nmol/mg protein, which seems to be the threshold of copper overload that C6 cells can withstand under the conditions used. This value is slightly higher than those reported previously for C6 glioma cells (20 nmol/mg) [22] and for cultured astrocytes (10 nmol/mg) [7].

Dispersions of CuO-NPs are known to release copper ions during storage of CuO-NPs [18, 19]. Analysis of the concentration of contaminating copper ions in the stored CuO-NP dispersion used for the current study revealed that not more than approximately 10% of total copper content of the dispersion represented ionic copper that was chelatable by BCS. As this free ionic copper in the CuO-NP dispersion has previously been connected to the observed toxicity of CuO-NPs [19, 21, 22], the contaminating ionic copper was extracellularly chelated by the membrane impermeable copper chelator BCS [24, 34] in a concentration that accounted to 20% of the total copper content. Physicochemical characterization of the CuO-NP dispersion in IB-BSA-BCS revealed that the presence of 20% BCS did not significantly

alter the average hydrodynamic diameter nor the zeta potential of the dispersed CuO-NPs.

Application of CuO-NPs to cultured glial cells in the absence of BCS caused a concentration-dependent increase in cellular copper content and a loss in cell viability, as previously reported for glial cells [7, 22]. These effects were not modulated by the presence of 20% BCS, demonstrating that accumulation of intact CuO-NPs by the cells, and not the uptake of copper ions, caused the observed copper accumulation and toxicity. For $CuCl_2$-treated cells a similar concentration-dependent copper accumulation and severe toxicity was observed, but those effects were drastically lowered by the presence of 20% BCS, demonstrating that under the conditions used BCS was even at a low molar ratio of 20% able to at least partially prevent copper accumulation and copper-induced toxicity from extracellular copper ions.

CuO-NPs and ionic copper are taken up by different transport mechanisms in glial cells. While copper ions are primarily taken up via copper transporters such as Ctr1 [40, 41], cellular NP uptake is likely to occur via endocytotic mechanisms [6, 42, 43]. As both processes are strongly affected by the temperature [7, 40, 44, 45], the lowering of the incubation temperature to 4 °C almost completely prevented copper accumulation und cell toxicity in cultured glial cells that had been treated with CuO-NPs or ionic copper.

BCS has a high affinity for copper ions and binds copper ions in a stoichiometry of 1 copper ion to 2 BCS molecules [34], but also the BSA present in the incubation medium is known as an excellent copper ion chelator [46, 47]. Therefore, it was expected that for the conditions used, the presence of extracellular BSA lowered the uptake and toxicity of ionic copper substantially. However, the concentration of BSA present (0.5 mg per mL) appears not to be sufficient to completely prevent copper accumulation after application of $CuCl_2$, explaining why the addition of BCS in a concentration of 20% already significantly lowered copper accumulation from ionic copper to values that did not cause toxicity in cultured glial cells. With increasing BCS concentration cellular copper accumulation was further lowered and a 2 times molar excess of BCS over copper completely prevented the cellular copper accumulation.

BCS will as charged compound not diffuse into intact cells. In addition, due to the formation of a Cu-BCS complex, the uptake of ionic copper in cultured glial cells is prevented in presence of BCS as reported previously [24, 32]. As the presence of 20% BCS did not affect the physiochemical properties and the accumulation of CuO-NPs by glial cells, the extracellular liberation of copper ions from the NPs during the incubation can be excluded as an extracellular source for copper accumulation and copper-induced toxicity. Only if 2 mM BCS had been co-incubated with 1 mM CuO-NPs, the cellular copper accumulation and the copper-induced toxicity were prevented. However, such conditions caused rapid and almost complete liberation of copper ions from the CuO-NPs as demonstrated by the formation of the high amounts of Cu-BCS complex which in turn prevented copper accumulation and toxicity.

Copper-induced toxicity has been connected with an enhanced formation of ROS via a Fenton-like reaction [48], as shown for copper-treated glial cells [7, 42] and other cell types [49, 50]. Only a low concentration of copper (100 µM) applied in the form of ionic copper ($CuCl_2$) or CuO-NPs caused severe ROS production in glial cells, which was not prevented in the presence of 20% BCS (data not shown). Thus, a persistence of elevated cellular ROS levels was observed even under the conditions where toxicity was completely prevented. This indicates that, while copper application causes elevated cellular oxidative stress, it is most likely not the primary cause for the observed copper-induced toxicity. Several studies have linked copper ion- and CuO-NP-induced toxicity to their interaction with and the inactivation of cellular biomolecules which subsequently impaired processes such as protein folding, protein aggregation, thiol cross-linking, enzymatic activity or lysosomal functions [6, 51–54]. Thus, oxidative stress may contribute only little to the severe adverse effect of a copper overload after exposure of glial cells to CuO-NPs.

In conclusion, application of the membrane-impermeable chelator BCS in a low 20% molar concentration compared to the copper applied as CuO-NPs in IB-BSA, allowed to chelate contaminating ionic copper and to study accumulation and toxicity of intact CuO-NPs in cultured glial cells. The results obtained demonstrate that the copper accumulation and copper-induced toxicity observed after application of CuO-NP dispersions to cultured glial cells are not mediated by contaminating copper ions but are rather a consequence of the uptake of intact CuO-NPs into the cells.

Liberation of metal ions is frequently observed for dispersions of metal-containing NPs and the discrimination between metal ion effects and NP-mediated effects is a severe problem [21, 55, 56]. Application of a low concentration of a non-membrane permeable chelator should also be considered as a strategy for cell experiments using other types of metal-containing NPs that leak metal ions. This may help also in other projects to discriminate between adverse effects on cultured cells of contaminating extracellular metal ions and the specific effects of accumulated NPs.

Acknowledgements Arundhati Joshi would like to thank the Hans-Böckler Foundation for a PhD fellowship at the Graduate School Nano-Competence at the University of Bremen, Germany.

Compliance with Ethical Standards

Conflict of interest The authors declare that they have no conflict of interest.

References

1. Chauhan M, Sharma B, Kumar R, Chaudhary GR, Hassan AA, Kumar S (2019) Green synthesis of CuO nanomaterials and their proficient use for organic waste removal and antimicrobial application. Environ Res 168:85–95
2. Khatami M, Alijani HQ, Sharifi I (2018) Biosynthesis of bimetallic and core–shell nanoparticles: their biomedical applications–a review. IET Nanobiotechnol 12:879–887
3. Kadiyala U, Kotov NA, VanEpps JS (2018) Antibacterial metal oxide nanoparticles: challenges in interpreting the literature. Curr Pharm Des 24:896–903
4. Titma T, Shimmo R, Siigur J, Kahru A (2016) Toxicity of antimony, copper, cobalt, manganese, titanium and zinc oxide nanoparticles for the alveolar and intestinal epithelial barrier cells in vitro. Cytotechnology 68:2363–2377
5. Líbalová H, Costa PM, Olsson M, Farcal L, Ortelli S, Blosi M, Topinka J, Costa AL, Fadeel B (2018) Toxicity of surface-modified copper oxide nanoparticles in a mouse macrophage cell line: Interplay of particles, surface coating and particle dissolution. Chemosphere 196:482–493
6. Zhang J, Zou Z, Wang B, Xu G, Wu Q, Zhang Y, Yuan Z, Yang X, Yu C (2018) Lysosomal deposition of copper oxide nanoparticles triggers HUVEC cells death. Biomaterials 161:228–239
7. Bulcke F, Thiel K, Dringen R (2014) Uptake and toxicity of copper oxide nanoparticles in cultured primary brain astrocytes. Nanotoxicology 8:775–785
8. Kukia NR, Abbasi A, Froushani SMA (2018) Copper oxide nanoparticles stimulate cytotoxicity and apoptosis in glial cancer cell line. Dhaka Univ J Pharm Sci 17:105–111
9. Vinardell M, Mitjans M (2018) Metal/metal oxide nanoparticles for cancer therapy. In: Goncalves G, Tobias G (eds) Nanooncology. Springer, Cham, pp 341–364
10. Zhou Y, Peng Z, Seven ES, Leblanc RM (2018) Crossing the blood-brain barrier with nanoparticles. J Control Release 270:290–303
11. Khalid S, Afzal N, Khan JA, Hussain Z, Qureshi AS, Anwar H, Jamil Y (2018) Antioxidant resveratrol protects against copper oxide nanoparticle toxicity in vivo. Naunyn-Schmiedeberg's Arch Pharmacol 391:1053–1062
12. Li X, Sun W, An L (2018) Nano-CuO impairs spatial cognition associated with inhibiting hippocampal long-term potentiation via affecting glutamatergic neurotransmission in rats. Toxicol Ind Health 34:409–421
13. Lian D, Chonghua Z, Wen G, Hongwei Z, Xuetao B (2017) Label-free and dynamic monitoring of cytotoxicity to the blood–brain barrier cells treated with nanometre copper oxide. IET Nanobiotechnol 11:948–956
14. Prabhu BM, Ali SF, Murdock RC, Hussain SM, Srivatsan M (2010) Copper nanoparticles exert size and concentration dependent toxicity on somatosensory neurons of rat. Nanotoxicology 4:150–160
15. Mahmoud A, Elif GE, Gül O (2016) Copper (II) Oxide nanoparticles induce high toxicity in human neuronal cell. Glob J Med Res 16:7–14
16. Conway JR, Adeleye AS, Gardea-Torresdey J, Keller AA (2015) Aggregation, dissolution, and transformation of copper nanoparticles in natural waters. Environ Sci Technol 49:2749–2756
17. Midander K, Wallinder IO, Leygraf C (2007) In vitro studies of copper release from powder particles in synthetic biological media. Environ Pollut 145:51–59
18. Midander K, Cronholm P, Karlsson HL, Elihn K, Möller L, Leygraf C, Wallinder IO (2009) Surface characteristics, copper release, and toxicity of nano-and micrometer-sized copper and copper (II) oxide particles: a cross-disciplinary study. Small 5:389–399
19. Semisch A, Ohle J, Witt B, Hartwig A (2014) Cytotoxicity and genotoxicity of nano-and microparticulate copper oxide: role of solubility and intracellular bioavailability. Part Fibre Toxicol 11:10–26
20. Jeong J, Kim S-H, Lee S, Lee D-K, Han Y, Jeon S, Cho W-S (2018) Differential contribution of constituent metal ions to the cytotoxic effects of fast-dissolving metal-oxide nanoparticles. Front Pharmacol 9:15–25
21. Wang D, Lin Z, Wang T, Yao Z, Qin M, Zheng S, Lu W (2016) Where does the toxicity of metal oxide nanoparticles come from: the nanoparticles, the ions, or a combination of both? J Hazard Mater 308:328–334
22. Joshi A, Rastedt W, Faber K, Schultz AG, Bulcke F, Dringen R (2016) Uptake and toxicity of copper oxide nanoparticles in C6 glioma cells. Neurochem Res 41:3004–3019
23. Cho W-S, Duffin R, Poland CA, Duschl A, Oostingh GJ, MacNee W, Bradley M, Megson IL, Donaldson K (2012) Differential pro-inflammatory effects of metal oxide nanoparticles and their soluble ions in vitro and in vivo; zinc and copper nanoparticles, but not their ions, recruit eosinophils to the lungs. Nanotoxicology 6:22–35
24. Chen S-H, Lin J-K, Liu S-H, Liang Y-C, Lin-Shiau S-Y (2007) Apoptosis of cultured astrocytes induced by the copper and neocuproine complex through oxidative stress and JNK activation. Toxicol Sci 102:138–149
25. Kim BH, Yang J, Lee D, Choi BK, Hyeon T, Park J (2018) Liquid-phase transmission electron microscopy for studying colloidal inorganic nanoparticles. Adv Mater 30:1703316
26. Michen B, Geers C, Vanhecke D, Endes C, Rothen-Rutishauser B, Balog S, Petri-Fink A (2015) Avoiding drying-artifacts in transmission electron microscopy: Characterizing the size and colloidal state of nanoparticles. Sci Rep 5:9793
27. Benda P, Lightbody J, Sato G, Levine L, Sweet W (1968) Differentiated rat glial cell strain in tissue culture. Science 161:370–371
28. Stapelfeldt K, Ehrke E, Steinmeier J, Rastedt W, Dringen R (2017) Menadione-mediated WST1 reduction assay for the determination of metabolic activity of cultured neural cells. Anal Biochem 538:42–52
29. Tulpule K, Hohnholt MC, Hirrlinger J, Dringen R (2014) Primary cultures of astrocytes and neurons as model systems to study the metabolism and metabolite export from brain cells. In: Hirrlinger J, Waagepetersen H (eds) Neuromethods: brain energy metabolism. Springer, New York, pp 45–72
30. Lowry OH, Rosebrough NJ, Farr AL, Randall RJ (1951) Protein measurement with the Folin phenol reagent. J Biol Chem 193:265–275
31. Chen L, Xue X, Jiang D, Yang J, Zhao B, Han XX, Mee Jung Y (2016) A turn-on resonance Raman scattering (BCS/Cu^{+}) sensor for quantitative determination of proteins. Appl Spectrosc 70:355–362
32. Bulcke F, Santofimia-Castaño P, Gonzalez-Mateos A, Dringen R (2015) Modulation of copper accumulation and copper-induced toxicity by antioxidants and copper chelators in cultured primary brain astrocytes. J Trace Elem Med Biol 32:168–176
33. Stark WJ (2011) Nanoparticles in biological systems. Angew Chem 50:1242–1258
34. Chen D, Darabedian N, Li Z, Kai T, Jiang D, Zhou F (2016) An improved Bathocuproine assay for accurate valence identification and quantification of copper bound by biomolecules. Anal Biochem 497:27–35
35. Arratia F, Olivares-Ferretti P, García-Rodríguez A, Marcos R, Carmona ER (2019) Comparative toxic effects of copper-based

nanoparticles and their microparticles in Daphnia magna by using natural freshwater media. New Zeal J Mar Fresh 53:460–469
36. Henson TE, Navratilova J, Tennant AH, Bradham KD, Rogers KR, Hughes MF (2019) In vitro intestinal toxicity of copper oxide nanoparticles in rat and human cell models. Nanotoxicology 13:795–811
37. Jurašin DD, Ćurlin M, Capjak I, Crnković T, Lovrić M, Babič M, Horák D, Vrček IV, Gajović S (2016) Surface coating affects behavior of metallic nanoparticles in a biological environment. Beilstein J Nanotechnol 7:246–262
38. Ortelli S, Costa AL, Blosi M, Brunelli A, Badetti E, Bonetto A, Hristozov D, Marcomini A (2017) Colloidal characterization of CuO nanoparticles in biological and environmental media. Environ Sci Nano 4:1264–1272
39. Geppert M, Petters C, Thiel K, Dringen R (2013) The presence of serum alters the properties of iron oxide nanoparticles and lowers their accumulation by cultured brain astrocytes. J Nanopart Res 15:1349–1364
40. Scheiber IF, Mercer JF, Dringen R (2010) Copper accumulation by cultured astrocytes. Neurochem Int 56:451–460
41. Tiffany-Castiglioni E, Qian Y (2001) Astroglia as metal depots: molecular mechanisms for metal accumulation, storage and release. Neurotoxicology 22:577–592
42. Bulcke F, Dringen R (2016) Handling of copper and copper oxide nanoparticles by astrocytes. Neurochem Res 41:33–43
43. Behzadi S, Serpooshan V, Tao W, Hamaly MA, Alkawareek MY, Dreaden EC, Brown D, Alkilany AM, Farokhzad OC, Mahmoudi M (2017) Cellular uptake of nanoparticles: journey inside the cell. Chem Soc Rev 46:4218–4244
44. Willmann W, Dringen R (2018) Monitoring of the cytoskeleton-dependent intracellular trafficking of fluorescent iron oxide nanoparticles by nanoparticle pulse-chase experiments in C6 glioma cells. Neurochem Res 43:2055–2071
45. Geppert M, Hohnholt MC, Thiel K, Nürnberger S, Grunwald I, Rezwan K, Dringen R (2011) Uptake of dimercaptosuccinate-coated magnetic iron oxide nanoparticles by cultured brain astrocytes. Nanotechnology 22:145101–145111
46. Masuoka J, Saltman P (1994) Zinc (II) and copper (II) binding to serum albumin. A comparative study of dog, bovine, and human albumin. J Biol Chem 269:25557–25561
47. Peters T, Blumenstock FA (1967) Copper-binding properties of bovine serum albumin and its amino-terminal peptide fragment. J Biol Chem 242:1574–1578
48. Scheiber IF, Mercer JF, Dringen R (2014) Metabolism and functions of copper in brain. Prog Neurobiol 116:33–57
49. Akhtar MJ, Kumar S, Alhadlaq HA, Alrokayan SA, Abu-Salah KM, Ahamed M (2016) Dose-dependent genotoxicity of copper oxide nanoparticles stimulated by reactive oxygen species in human lung epithelial cells. Toxicol Ind Health 32:809–821
50. Angelé-Martínez C, Nguyen KVT, Ameer FS, Anker JN, Brumaghim JL (2017) Reactive oxygen species generation by copper (II) oxide nanoparticles determined by DNA damage assays and EPR spectroscopy. Nanotoxicology 11:278–288
51. Huang Y-W, Cambre M, Lee H-J (2017) The toxicity of nanoparticles depends on multiple molecular and physicochemical mechanisms. Int J Mol Sci 18:2702–2715
52. Chang Y-N, Zhang M, Xia L, Zhang J, Xing G (2012) The toxic effects and mechanisms of CuO and ZnO nanoparticles. Materials 5:2850–2871
53. Macomber L, Imlay JA (2009) The iron-sulfur clusters of dehydratases are primary intracellular targets of copper toxicity. Proc Natl Acad Sci 106:8344–8349
54. Saporito-Magriñá CM, Musacco-Sebio RN, Andrieux G, Kook L, Orrego MT, Tuttolomondo MV, Desimone MF, Boerries M, Borner C, Repetto MG (2018) Copper-induced cell death and the protective role of glutathione: the implication of impaired protein folding rather than oxidative stress. Metallomics 10:1743–1754
55. Noventa S, Hacker C, Rowe D, Elgy C, Galloway T (2018) Dissolution and bandgap paradigms for predicting the toxicity of metal oxide nanoparticles in the marine environment: an in vivo study with oyster embryos. Nanotoxicology 12:63–78
56. Djurišić AB, Leung YH, Ng AM, Xu XY, Lee PK, Degger N, Wu R (2015) Toxicity of metal oxide nanoparticles: mechanisms, characterization, and avoiding experimental artefacts. Small 11:26–44